A Feasibility Study for 4H-SiC Diode Detectors as Neutron Flux Monitors in the GT-MHR

Behrooz Khorsandi,[*1] Mehdi Reisi-Fard,[1] Thomas E. Blue,[1] Jonathan Kulisek[1], Benone Lohan,[2] and Don W. Miller[1]
[1]*The Ohio State University, Nuclear Engineering program, Columbus, Ohio, USA*
[2]*Westinghouse Electric Company, Monroeville, Pennsylvania, USA*

Abstract

This paper presents an integrated study regarding the feasibility of using 4H-SiC semiconductor neutron diode detectors in the GT-MHR core. The goal of the study is to introduce a method to identify locations in the GT-MHR, where the detector count rate is acceptably high and the detector life-time may be acceptably long. The modeling methods that we have used to determine the neutron count rate and the rate of displacement damage are discussed.

KEYWORDS: GT-MHR, silicon carbide, count rate, MCNP

1. Introduction

There is considerable interest in developing neutron monitoring systems for next generation reactors, such as the Gas Turbine-Modular Helium Reactor (GT-MHR) [1]. The GT-MHR has been designed to work at high temperatures, with an outlet coolant temperature of about 850^{o}C, during normal full power operation. In comparison, commercial light water reactors have an outlet coolant temperature of about 300^{o}C, during normal full power operation. Due to the harsh environment in the GT-MHR, neutron flux monitors for light water reactors may not be appropriate for use in the GT-MHR. A new type of semiconductor radiation detector is under development based on silicon carbide (SiC), specifically 4H-SiC, technology. As a semiconductor material, 4H-SiC has some remarkable properties that make it a potentially useful material with which to form semiconductor neutron diode detectors for high temperature and high fluence applications. 4H-SiC has a large bandgap, is radiation hard and is nearly chemically and neutronically inactive. Semiconductor neutron diode detectors formed from 4H-SiC Schottky diodes, possess, in addition to the material characteristics of 4H-SiC, characteristics common to semiconductor diode detectors, which make semiconductor diode detectors well-suited for use as power monitors for nuclear reactors. Among these characteristics are small size and the potential for pulse mode operation at high counts rates.

Despite being radiation hard, a 4H-SiC neutron diode detector may not be able to withstand the extreme conditions in the GT-MHR. The energetic projectile particles (core neutrons and tritons coming from a ^{6}LiF radiator that is a part of the detector package), may collide with Si and C atoms and transfer energy to them. If the transferred energy exceeds some threshold values (E_ds), the Primary Knock-on Atoms (PKAs) move from

[*] Corresponding author, Tel. 614-404-7352, E-mail: khorsandi.1@osu.edu

their original positions, creating displacement damage defects. With increasing neutron fluence, the accumulation of defects destroys the 4H-SiC crystalline structure, thus degrading the performance of the detector. In addition, prolonged exposure to the very high temperatures in the reactor, may cause the detector Ohmic and Schottky contacts to fail.

2. Design and Modeling

2.1 Detector and Electronics Channel Design

Per the design of Westinghouse Electric Company [4], the SiC neutron detector package is based on a Schottky diode that relies on the detection of tritons that are emitted from a LiF radiator layer with 90% ^{6}Li enrichment. The physical configuration of the detector package is shown in Fig. 1. Its design includes the following material layers with the indicated layer thicknesses: 1-μm LiF, 8-μm Al (to shield the SiC from the emitted alpha particles), 1-μm Au Schottky contact, 10-μm depleted SiC (n-type SiC) and 300-μm substrate SiC (n^{+}-SiC). The SiC diode detector responds to fast neutrons that interact with Si and C atoms, as well as to the tritons that are born in the LiF. For the neutron events and tritons to be recorded, the recoiling Si and C atoms and the tritons must create, in the diode's depleted SiC region, a number of electron and hole pairs that is above some user controlled discrimination level that is set high enough to preclude gamma ray events from being recorded.

Figure 1: SiC neutron diode detector package geometry. The detector is sensitive to fast neutrons that interact in the SiC and to tritons that are born in the LiF radiator. For events to be recorded, a sufficient number of electron and hole pairs must be created in the depleted region of the SiC.

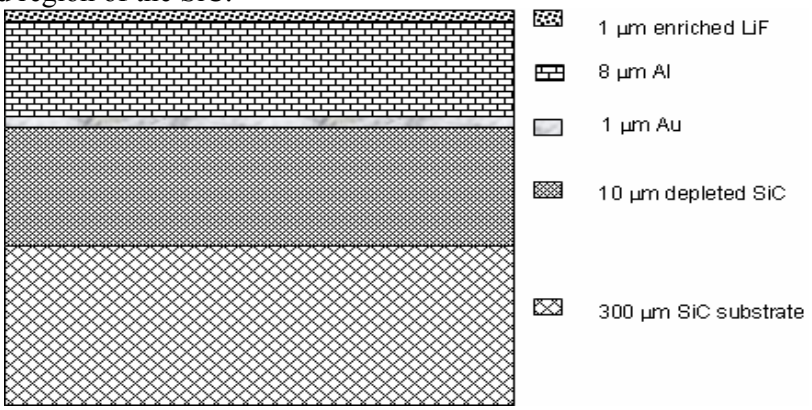

An important component of the detector and electronics channel design was to predict the response of the detector channel to neutron-induced (n,alpha) interactions in the ^{6}LiF radiator that is a part of the detector package. The physical configuration of the detector package was modeled using TRIM [2]. Its electronic configuration was modeled using MATLAB [3]. The electronic configuration of the detector channel is shown schematically in Fig. 2, as it was built. The schematic diagram of the MATLAB model of the detector channel is identical to Fig. 2, with the exceptions that the matching impedance circuit, the power supply, and the signal splitter are not present in the schematic diagram of the model, since these elements of the channel are assumed to perform their functions

ideally. Using TRIM and MATLAB, the formation of electronic pulses in the detector was simulated for isotropic emission of tritons in the radiator. From these simulations, we predicted the fraction of tritons that are born in the ^{6}LiF radiator, which result in recorded pulses, as a function of pulse height discriminator voltage. We also predicted the fraction of the triton induced pulses that exceed the discriminator voltage, which will not be counted, because of discriminator dead time.

Figure 2: Schematic diagram of the SiC detector neutron monitoring channel, as it was built.

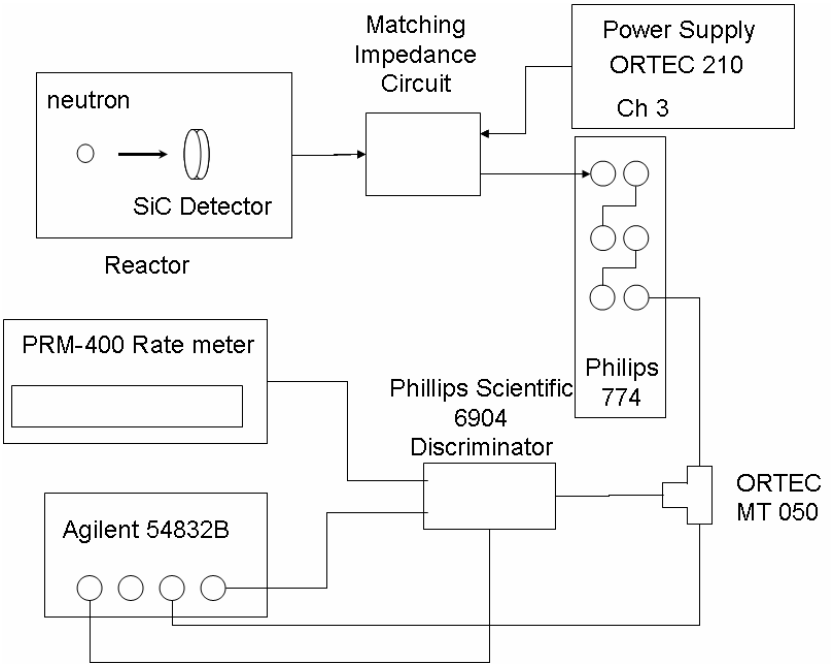

A second important component of the detector and electronics channel design was to predict the neutron-induced (n,alpha) reaction rate within the ^{6}LiF radiator for various in-core and ex-core detector locations. A He-cooled capsule was designed to contain the detectors for in-core detector locations. Figure 3 presents transverse and longitudinal views of the GT-MHR core, with the detector capsule locations identified in the figure [5]. It should be noted that the detector capsules are not a part of the original GT-MHR design and have been added by us, for the purposes of this analysis. The main objective of the capsule is to maintain the SiC detector packages at the optimum operating temperature to minimize detector damage. The energy-dependent neutron flux was calculated using MCNP5, for several axial locations within the capsule, for several hypothetical capsule radial locations. Based on the calculated energy-dependent neutron flux, the neutron-induced (n,alpha) reaction rate, within the ^{6}LiF radiator, was calculated.

In Fig. 3, the capsules radial and azimuthal positions are shown in the schematic. For purposes of brevity, our analysis methods, and the results of our methods of analysis, are presented in this paper for only one in-core radial location for the capsule (R=153 cm), the location of the capsule that is closest to the fuel annulus. The axial locations of SiC detectors, for which results are presented in this paper (layers 3, 5 and 8), are shown in the right schematic, as blue circles.

Figure 3: Transverse and longitudinal views of the MCNP GT-MHR model.

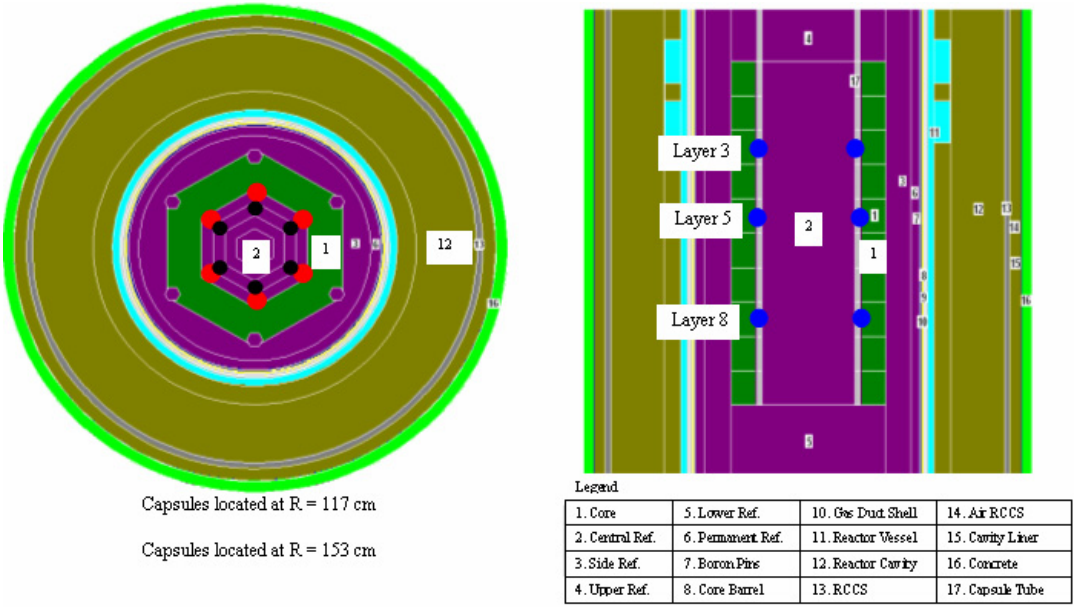

2.2 Damage Modeling

With the SiC neutron diode detector, one estimates the neutron flux inside the reactor by monitoring the triton count rate due to the neutron-induced (n,alpha) reaction rate within the 6LiF radiator. Also one unavoidably records events that are a consequence of neutrons colliding to produce SiC Primary Knock-on Atoms (PKAs) within the detector. The detector is unavoidable damaged as a consequence of registration of the triton and PKA counts. The tritons and PKAs collide with other SiC atoms, creating a cascade of defects, including vacancies, interstitials and antisites. Displacement damage modeling is an important step in predicting, and controlling, the number of defects.

There are four origins for the projectile particles that initiate displacement damage cascades in the SiC diode detector packages of the design that is shown in Fig. 1. They are: 1) tritons that are emitted in the LiF layer with an initial energy of 2.73MeV; 2) Si- and C-PKAs that are created by neutron scattering reactions; 3) 1.33keV-^{29}Si recoils from ^{28}Si(n,γ)^{29}Si reactions; and 4) 2.76keV-^{13}C recoils from ^{12}C(n,γ)^{13}C reactions. The damage created in the SiC layers by these projectiles, except tritons, is uniformly distributed over the SiC volume, since the detectors are thin and neutrons do not have a specific range in materials. On the contrary, the damage created by tritons is non-uniform, since tritons have a finite range in the SiC layers and are emitted in a geometry which consists of finite planes.

Damage in SiC detectors (for several axial locations within the capsule, for the several hypothetical capsule locations for which the count rate was determined) was characterized using two terms: 1) The 1 MeV equivalent neutron flux in SiC ($\phi^{Total}_{eq,1MeV,SiC}$) [6], and 2) The number of vacancies per atom per fluence (N_{VPA}/Φ). $\phi^{Total}_{eq,1MeV,SiC}$ is a well-known and appropriate function to compare the displacement damage rate at low temperatures in SiC, for fluxes with different energy spectra; however, damage resulting from tritons is not included in the $\phi^{Total}_{eq,1MeV,SiC}$ definition. The calculation of N_{VPA}/Φ is an

important step, for a more advanced analysis to determine the evolution of the concentration of defects of various species (such as vacancies), as a function of temperature, over a reactor refueling cycle, as a consequence of displacement damage creation and recovery. The advantage of N_{VPA}/Φ over $\phi^{Total}_{eq,1MeV,SiC}$ is that the damage caused by all projectiles, with the origins cited in the above paragraph, is included in N_{VPA}/Φ.

To calculate N_{VPA}/Φ, we proceeded as follows. First, we used the PTRAC card in MCNP5 [7] to determine the fraction of neutrons which strike Si or C atoms as they pass through the detector, for neutrons of various energies. Then we wrote a C-program to extract the neutron characteristics (energy, position and direction cosines) before and after each collision, as well as the type of the PKAs, from the PTRAC files that were created by MCNP5. Using conservation of energy, the PKA energy and direction cosines were determined using the MCNP5 PTRAC output for the scattered neutrons. The output of the C-program was used as an input for the TRIM and MARLOWE [8] codes. These binary-collision approximation (BCA) codes were, in turn, used to estimate the number of C- and Si-defects that were created as a consequence of irradiation with neutron fluences of various neutron energies.

3. Results

TRIM and MATLAB simulations show that, provided that the detector is located in a position with a sufficiently high thermal neutron flux, with a voltage sensitive preamplifier, the detector is able to count tritons at a rate of approximately $4*10^7$ cps with less than 10% count loss. This high count rate allows the neutron flux to be monitored effectively over a wide dynamic range. The extent of the dynamic range depends upon the required accuracy at the low count rate limit of the dynamic range. This accuracy is dictated by the certainty one demands of the signal for initiating control actions, such as initiating a scram. The relationship between count rate, counting time, and monitor accuracy is established by Poisson counting statistics. The time that is available to initiate control actions for the GT-MHR is not known to us. We have assumed in this analysis, for the purposes of specificity, that statistics, which are sufficiently good to initiate control actions, must be obtained within a counting time of 1 second.

Figure 5 shows two curves. The curve with the diamond-shaped data points shows the calculated accuracy of the monitoring channel over its dynamic range, assuming the counting system yields a count rate of $4*10^7$ cps at 100% power and that the counting time is 1 second. Due to capability of the power monitoring system to count at high count rates, for a detector counting interval of one second, the flux monitoring channel can operate with better than 5% accuracy for reactor powers as low as 10^{-3} % of full power. As one can see from Figure 5, the curve of detector accuracy versus reactor power is concave upward, with a minimum at approximately 1% of full power.

At high power, the accuracy of the channel is restricted by the count loss due to the discriminator dead time and, at low powers, the accuracy is limited by statistical error due to the low count rate. The inaccuracy of the counting channel, at high powers, is a systematic error, which can be corrected, with an appropriate model of dead time count loss. In contrast, the inaccuracy of the counting channel, at low powers, is fundamental and cannot be corrected. In this paper, we assume that the inaccuracy at high powers due to discriminator dead time count loss can be adequately corrected. We arbitrarily assume, for the purposes of illustration, that the upper limit for the fundamental inaccuracy of the counting system at low powers is 5%. Then for the detector channel that is described

above (with a count rate of $4*10^7$ cps at 100% power and a counting time of 1 second), the dynamic range covers five orders of magnitude and the neutron flux can be monitored from 10^{-3} % to 100% of full power with an acceptable uncertainty.

The second curve in Figure 5 (the curve with the square data points) shows the calculated accuracy of the monitoring channel over its dynamic range, assuming, as before, that the counting time is 1 second; but assuming, in contrast to the previous assumption, that the counting system yields a count rate of only $6.4*10^5$ cps at 100% power. As one might expect the curve of detector accuracy versus reactor power is shifted to higher powers by slightly less than two orders of magnitude, reflecting the change in count rate at 100% power by slightly less than two orders of magnitude. Correspondingly, assuming that the limits on inaccuracy of the detector channel are unchanged at low power (5%), the dynamic range of the detector channel is reduced by a little less than two orders of magnitude, and extends from approximately $5*10^{-2}$ % to 100% of full power.

Equation 1 presents a formula for the relationship between the detector dynamic range and parameters that are assumed in our calculations, such as the required accuracy of the counting system at the lower limits of its dynamic range and the counting time. Equation 1 assumes that the detector behaves in a non-paralyzable manner at high count rates. Our implementation of the Simulink model of the detector channel does not restrict the modeled count loss to being either paralyzable or non-paralyzable , but instead reflects the count rate limitation of the discriminator in combination with the modeled detector, cable, and amplifiers. Although Equation 1 does not perfectly reflect the details of our modeling, it is consistent with the general trends of our modeling. For example, for the case that the counting system yields a count rate of only $6.4*10^5$ cps at 100% power, then f_L=0.2% and $r_H/r_L=1.6*10^3$.

$$\frac{r_H}{r_L} = \frac{\frac{f_L}{\tau(1-f_L)}}{\frac{1}{t_s\varepsilon^2}} = \frac{t_s\varepsilon^2 f_L}{\tau(1-f_L)} \qquad \text{Equation 1}$$

r_H : Highest allowable count rate
r_L : Lower limit for count rate
τ : Pulse pair resolution of the discriminator
f_L : Acceptable fraction of counts lost
t_s : Counting time required to initiate a reactor SCRAM
ε : Fractional error acceptable in a SCRAM signal

As mentioned above, in our calculations, we assumed that the detector counting interval is one second. If the detector needs to respond faster, the counting channel becomes less accurate at low powers, and, as it can be seen from Equation 1, the dynamic range of the detector decreases in proportion to t_s. In addition, it can be seen from Equation 1 that the required channel accuracy, at low powers, enters the expression for the dynamic range quadratically in its numerator.

Figure 4: The accuracy of the neutron flux monitoring channel as a function reactor power.

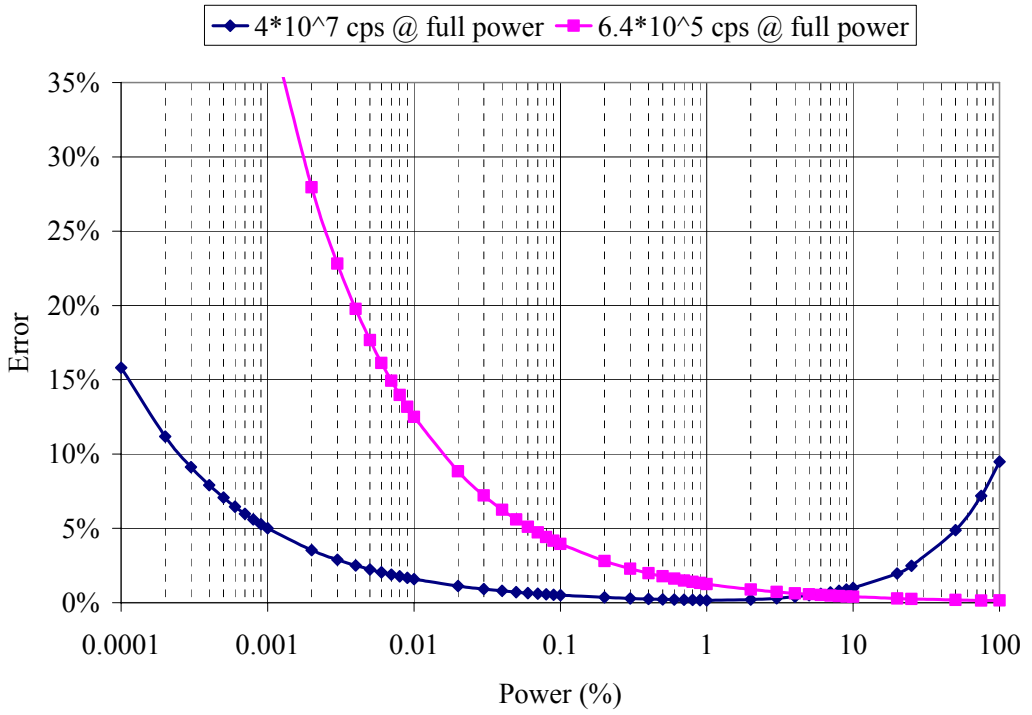

Besides the statistical error and the error due to the discriminator dead time, the ^{6}Li burn up may cause an additional error at the end of the reactor cycle. Also, although the electronic channel is able to process count rate of $4*10^{7}$, based on our MCNP simulations, the maximum achievable count rate is less than $4*10^{7}$, due to the limitation on the detector sensitivity.

Neutron flux energy spectra within the capsule located at R=153 cm, for three axial layers (layers 3, 5 and 8) are shown in Figure 5. As it can be seen in this figure, the three spectra are very nearly equal. The value of $\phi^{Total}_{eq,1MeV,SiC}$ and the total neutron flux, averaged over the three locations, corresponding to a triton count rate of approximately $6.4*10^{5}$ cps (an efficiency of 0.39 is applied to the (n,alpha) reaction rate in the ^{6}LiF radiator) is approximately $2.0*10^{13}$ $cm^{-2}s^{-1}$ and $4.4*10^{13}$ $cm^{-2}s^{-1}$, respectively. The detector count rate (of $6.4*10^{5}$ cps at full power) limits the dynamic range to slightly more than three orders of magnitude, as shown in Figure 4.

Figure 5: The differential neutron energy spectrum for three locations in the central reflector of GT-MHR central, close to the fuel elements.

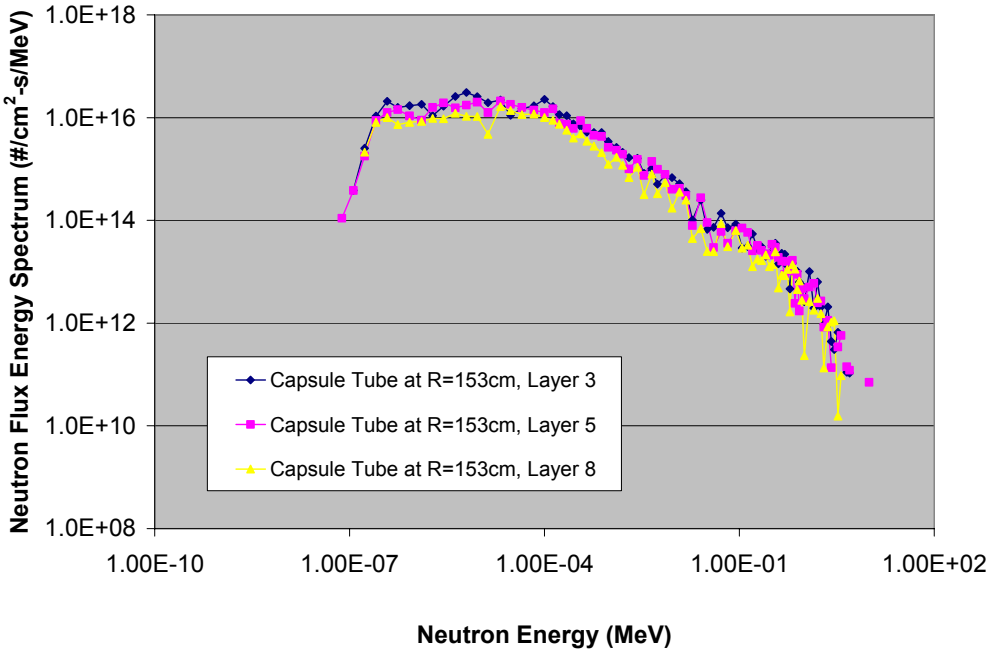

The corresponding predicted value of N_{VPA}/Φ is $4.4*10^{-22}$ cm^2. For a reactor refueling cycle (15.7 months), N_{VPA} for the stated averaged $\phi^{Total}_{eq,1MeV,SiC}$ is around 0.77. This means that, on average, 77% of the atoms comprising SiC will be displaced from their original sites, creating vacancies; however, most of the vacancies will disappear in a very short period of time, due to annealing. N_{VPA} for other GT-MHR locations, which are further from fuel elements (R=117cm), would be less than 0.06 for a 15.7 month reactor refueling cycle. At those locations, the SiC semiconductor has more chance to survive a reactor refueling cycle; however the total count rate may be smaller.

4. Conclusion

The goal of this paper was introduce a method with which to analyze the potential of SiC semiconductor diode detectors as in-core neutron power monitors for the GT-MHR. An analysis was presented with an example counting time required to initiate a reactor SCRAM (1 second) and an example acceptable fractional error in a SCRAM signal (5%). We found that, with these example counting times and fractional errors, with a voltage sensitive preamplifier channel operating at its upper count rate limit, the neutron flux can be effectively monitored over a dynamic range extending from 10^{-3} % to 100% of full power. However, we also found that, for the detector that was analyzed, at R=153 the upper count rate limit of the voltage sensitive preamplifier channel is not achieved. We have assessed the neutron induced damage rate in SiC, at full power and at low temperatures, using the 1 MeV equivalent neutron flux in SiC. The predicted value of $\phi^{Total}_{eq,1MeV,SiC}$, for detectors located in a capsule tube at R=153 cm, is approximately $2.0*10^{13}$ cm^{-2}s^{-1}.

In summary, the required response time and accuracy of the monitoring system must be specified to pursue the monitoring system design further. The results that are presented in

this paper do not account for annealing of damage. Modeling and experiments need to be done to determine how temperature and time impact the concentration of defects, such as vacancies.

Acknowledgements

This material is based upon work supported by the US Department of Energy under the NERI program Award No. DE-FG-07-02SF22620 and NERI Project Number 02-207. Any opinions, findings, and conclusions or recommendations expressed in this material are those of the authors and do not necessarily reflect the views of the Department of Energy.

References

1) General Atomics, "Gas Turbine-Modular Helium Reactor (GT-MHR) conceptual design description report," Project No. 7658, (July 1996).
2) F.J. Ziegler, "SRIM-2003," Nuclear Instruments and Methods in Physics Research, B, No. 219-220, 1027 (2004).
3) The MathWorks, Inc., 3 Apple Hill Drive, Natick, MA 01760.
4) A. R. Dulloo, et al., "The Neutron Response of Miniature Silicon Carbide Semiconductor Detector," Nuclear Instruments and Methods in Physics Research A 422, 47 (1999).
5) B. Lohan, M. Reisi-Fard, B. Khorsandi, A. Orosz , "SiC diode detectors as in-core neutron power monitors for the GT-MHR," Class Group Project, The Ohio State University, Nuclear Engineering Program, (Dec. 2003).
6) ASTM E722-94: Characterization Neutron Energy Fluence Spectra in Terms of an Equivalent Monoenergetic Neutron Fluence for Radiation-Hardness Testing of Electronics, Reapproved in 2002.
7) R.A. Forster, et al, "MCNP Version 5," Nuclear Instruments and Methods in Physics Research, B, No. 213, 82, (2004).
8) M.T. Robinson, "MARLOWE binary collision cascade simulation program, Version 15a, a guide for users," (Sept. 1, 2001).